

Excitation of the collective states in a three- qubit system

Ya. S. Greenberg^{1,*} and A. A. Shtygashev¹

¹*Novosibirsk State Technical University, Novosibirsk, Russia*

(Dated: January 15, 2020)

In the present paper, we have proposed the experimentally achievable method for the characterization of the collective states of qubits in a linear chain. We study temporal dynamics of absorption of a single-photon pulse by three interacting qubits embedded in a one-dimensional waveguide. Numerical simulations were performed for a Gaussian-shaped pulse with different frequency detunings and interaction parameters between qubits. The dynamic behavior of the excitation probability for each qubit is investigated. It was shown that the maximum probability amplitudes of excitation of qubits are reached when the frequency of external excitation coincides with the frequency of excitation of the a corresponding eigenstate of the system. In this case, the the magnitude of the probability amplitude of each qubit in the chain unambiguously correlates with the contribution of this qubit to the corresponding collective state of the system, and the decay of these amplitudes are determined by the resonance width arising from the interaction of the qubit with the photon field of the waveguide. Therefore, we show that the pulsed harmonic probe can be used for the characterization of the energies, widths, and the wavefunctions of the collective states in a one-dimensional qubit chain.

I. INTRODUCTION

Quantum bits (qubits) are at the heart of quantum information processing schemes. Currently, solid-state qubits, and in particular the superconducting ones, seem to satisfy the requirements for being the building blocks of viable quantum computers, since they exhibit relatively long coherence times, extremely low dissipation, and scalability. Furthermore, the coupling between qubits has successfully been achieved that was followed by the construction of multiple-qubit logic gates and the implementation of several algorithms. Most of the information protocols in qubit systems are based on a train of recording and readout pulses. Mainly, the investigations are restricted to the pulsed excitation of single-qubit [1–6] or two-qubit systems [7–9]. However, the existing quantum processors consist of at least several tens of qubits [10]. Therefore, the study of the pulse excitation of multiqubit structures is of certain interest. As shown in [11], the behavior of multi-qubit structures under pulsed excitation has important features due to the interaction of a photon with collective multiparticle states. This interaction leads to such interesting physical effects as photon blockade, Fano interference, quantum entanglement, and superradiation radiation. In the present work, we investigate the dynamic behavior under pulsed excitation of a linear chain consisting of three qubits interacting with the photon field in a one-dimensional waveguide. In principle, our method can be extended to a linear chain of an arbitrary number of qubits. Here we have focused our study on three-qubit chain because for the energy spectrum of this system a simple analytical solution can be obtained. This will allow us to attribute a clear physical meaning to certain aspects of the dynamic behavior of the qubit excitation amplitudes. In contrast to [11], where a chain of real atoms was studied, here we consider superconducting qubits, which, unlike real atoms, have a technological spread in their parameters (for example, the excitation energies of qubits differ in principle from each other).

Besides, the excitation energy of each qubit can be individually tuned through external circuits. Another difference is that we take into account the direct interaction between qubits -the interaction of the Ising type between the nearest neighbors. This interaction leads to the formation of collective quasistationary states, the width of which is determined by the interaction of each qubit with the photon field of the waveguide. A numerical simulation was performed for a Gaussian-shaped packet with different parameters of frequency detuning and interaction between qubits. The dynamic behavior of the excitation probability of each qubit is investigated. It is shown that pulsed excitation makes it possible to identify collective states of the system. The magnitude of the excitation amplitude of each qubit in the chain is uniquely correlated with the contribution of this qubit to the corresponding stationary state of the system. The damping of these amplitudes is determined by the resonance widths of the quasistationary states. The article is organized as follows. In the first section, we consider a linear chain of three qubits that interact with each other according to the nearest neighbor Ising model. The wave functions and the energy spectrum of this system have been found. The dependence of the parameters of stationary states on the degree of non-identity of qubits has also been investigated. In the second section, the effective Hamiltonian of a 3-qubit system is investigated with account for spontaneous emission into the waveguide. In the third section, the Wigner-Weisskopf approximation, and a single-photon basis were used to obtain the differential equations for the amplitudes of excitation of individual qubits. The fourth section presents the results of numerical simulations of the excitation amplitudes of individual qubits under external excitation. It was shown that the magnitude of the excitation amplitude of each qubit in the chain uniquely correlates with the contribution of this qubit to the corresponding stationary state of the system, and the damping of these amplitudes is determined by the resonance width arising due to the interaction of the qubit with the photon field of the waveguide.

*Electronic address: greenberg@risp.ru

II. THREE INTERACTING QUBITS. WAVE FUNCTIONS AND THE ENERGY SPECTRUM.

We consider a linear chain of three equally spaced qubits which are located at the points $x_1 = -d, x_2 = 0, x_3 = +d$. Every qubit can be either in the excited, $|e\rangle$ or the ground state $|g\rangle$. The Hamiltonian which accounts for the interaction between nearest neighbor qubits is (we use units where $\hbar = 1$ throughout this paper):

$$H_0 = \frac{1}{2} \sum_{n=1}^3 \left(1 + \sigma_z^{(n)} \right) \Omega_n - J(\sigma_1^+ \sigma_2 + \sigma_2^+ \sigma_1 + \sigma_3^+ \sigma_2 + \sigma_2^+ \sigma_3) \quad (1)$$

where Ω_n -qubit excitation frequency, J -interqubit coupling, $\sigma_n^+ = |e_n\rangle \langle g_n|$, $\sigma_n = |g_n\rangle \langle e_n|$ are raising and lowering Pauli operators, and $\sigma_z^{(n)} |e_n\rangle = |e_n\rangle$, $\sigma_z^{(n)} |g_n\rangle = -|g_n\rangle$. Here we assume that J is not a photon mediated coupling. In superconducting circuits with on-chip embedded qubits, the interqubit coupling J is controlled technologically, so that the coupling between, say, first and third qubit may be absent no matter how close they are in real space. Below we consider single photon approximation with the only one qubit in the chain being excited. Therefore, we will limit Hilbert space to three vector states:

$$|1\rangle = |e_1 g_2 g_3\rangle, |2\rangle = |g_1 e_2 g_3\rangle, |3\rangle = |g_1 g_2 e_3\rangle \quad (2)$$

The wave function is taken as a superposition of the vector states (2):

$$\Psi_i = c_1^{(i)} |1\rangle + c_2^{(i)} |2\rangle + c_3^{(i)} |3\rangle, \quad (i = 1, 2, 3) \quad (3)$$

From Schrodinger equation, $H_0 \Psi = E \Psi$ we obtain a linear system which allows us to find the energies and the superposition coefficients c_i of our system:

$$\begin{pmatrix} \Omega_1 - E & -J & 0 \\ -J & \Omega_2 - E & -J \\ 0 & -J & \Omega_3 - E \end{pmatrix} \begin{pmatrix} c_1 \\ c_2 \\ c_3 \end{pmatrix} = 0 \quad (4)$$

From (4) we obtain the equation for the energies:

$$E^3 - a_2 E^2 - a_1 E - a_0 = 0 \quad (5)$$

where $a_2 = \Omega_1 + \Omega_2 + \Omega_3$, $a_1 = 2J^2 - \Omega_3 \Omega_2 - \Omega_3 \Omega_1 - \Omega_2 \Omega_1$, $a_0 = \Omega_1 \Omega_2 \Omega_3 - (\Omega_1 + \Omega_3) J^2$. If all qubits are identical ($\Omega_1 = \Omega_2 = \Omega_3 = \Omega$) we obtain from (5) the energies of the system:

$$\begin{aligned} E_1 &= \Omega - \sqrt{2}J \\ E_2 &= \Omega \\ E_3 &= \Omega + \sqrt{2}J \end{aligned} \quad (6)$$

The superposition coefficients c_i are being calculated from (4) taking into account the normalization:

$$|c_1^{(i)}|^2 + |c_2^{(i)}|^2 + |c_3^{(i)}|^2 = 1, \quad (i = 1, 2, 3) \quad (7)$$

Finally, the wave functions are as follows. For the lowest energy $E_1 = \Omega - \sqrt{2}J$

$$\Psi_1 = \frac{1}{2} |1\rangle + \frac{\sqrt{2}}{2} |2\rangle + \frac{1}{2} |3\rangle \quad (8)$$

For $E = \Omega$

$$\Psi_2 = \frac{1}{\sqrt{2}} |1\rangle + 0 |2\rangle - \frac{1}{\sqrt{2}} |3\rangle \quad (9)$$

and for the highest energy $E_3 = \Omega + \sqrt{2}J$

$$\Psi_3 = \frac{1}{2} |1\rangle - \frac{\sqrt{2}}{2} |2\rangle + \frac{1}{2} |3\rangle \quad (10)$$

It is noteworthy that for identical qubits the superposition coefficients c_i do not depend on the coupling parameter J . The wave functions (8, 9, 10) are the collective states of a three-qubit chain which is given by the Hamiltonian (1). Unlike the real atoms, superconducting qubits are intrinsically not identical due to technological scattering of their parameters. The excitation energy of every qubit in a chain can moreover be adjusted to any value by an external circuit. Below, we consider the situation when the excitation frequency of one of the qubit is different from that of the other two qubits. Therefore, we take the first and the third qubit as identical ($\Omega_1 = \Omega_3 = \Omega$), while the excitation frequency of the second qubit is Ω_2 . A direct calculation of the matrix determinant (4) yields the following result:

$$E_1 = \Omega + \frac{\Delta}{2} - \frac{1}{2} \sqrt{\Delta^2 + 8J^2} \quad (11)$$

$$E_2 = \Omega \quad (12)$$

$$E_3 = \Omega + \frac{\Delta}{2} + \frac{1}{2} \sqrt{\Delta^2 + 8J^2} \quad (13)$$

where $\Delta = \Omega_2 - \Omega$.

For eigen energies E_1 and E_3 the superposition coefficients are as follows:

$$c_1^{(1)} = c_3^{(1)} = \frac{J}{\sqrt{2J^2 + 0.25(\sqrt{\Delta^2 + 8J^2} - \Delta)^2}}; \quad (14)$$

$$c_1^{(3)} = c_3^{(3)} = \frac{J}{\sqrt{2J^2 + 0.25(\sqrt{\Delta^2 + 8J^2} + \Delta)^2}}$$

$$c_2^{(1)} = \frac{1}{2} \frac{-\Delta + \sqrt{\Delta^2 + 8J^2}}{\sqrt{2J^2 + 0.25(\sqrt{\Delta^2 + 8J^2} - \Delta)^2}}; \quad (15)$$

$$c_2^{(3)} = -\frac{1}{2} \frac{\Delta + \sqrt{\Delta^2 + 8J^2}}{\sqrt{2J^2 + 0.25(\sqrt{\Delta^2 + 8J^2} + \Delta)^2}}$$

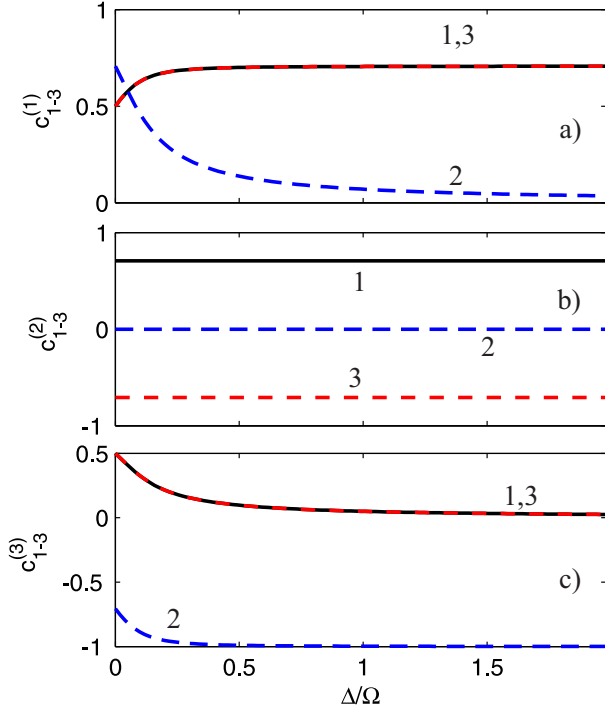


FIG. 1: Dependence of superposition coefficients (14,15) on Δ/Ω for $J/\Omega = 0.05$. The numbers on the panels correspond to superposition coefficients: 1- $c_1^{(i)}$ (black), 2- $c_2^{(i)}$ (blue), 3- $c_3^{(i)}$ (red).

For the second stationary state E_2 , superposition coefficients coincide with those in (9). The dependence of superposition coefficients on the parameter Δ/Ω is shown in Fig. 1. For the first energy state $|E_1\rangle$ all three coefficients $c_i^{(1)}$ become equal at the point $\Delta = J$ (panel a) in Fig. 1).

As is follows from (14,15), it results in the formation at that point of a maximally entangled state $|E_1\rangle = \frac{1}{\sqrt{3}}(|e_1g_2g_3\rangle + |g_1e_2g_3\rangle + |g_1g_2e_3\rangle)$. At this point, the second state $|E_2\rangle$ remains unaltered (9) while for the third state we have $|E_3\rangle = \frac{1}{\sqrt{6}}|e_1g_2g_3\rangle - \frac{2}{\sqrt{6}}|g_1e_2g_3\rangle + \frac{1}{\sqrt{6}}|g_1g_2e_3\rangle$. It can also be seen from ((14,15)) that as the detuning is increased ($\Delta/J \gg 1$) the first state transforms to a symmetrical entangled superposition $|E_1\rangle = \frac{1}{\sqrt{2}}(|e_1g_2g_3\rangle + |g_1g_2e_3\rangle)$, the third state is factorized $|E_3\rangle = -|g_1e_2g_3\rangle$ while the second state (9), remains unaltered. Below, we show that under pulsed excitation of a qubit chain, all these features emerge in the excitation spectrum of the qubit probability amplitudes.

III. PHOTON MEDIATED INTERACTIONS BETWEEN QUBITS

Spontaneous emission of qubits gives rise to the interqubit coupling via the photon field in a waveguide. This interaction can be described by the effective non-Hermitian Hamiltonian [12]:

$$\langle m|H_{eff}|n\rangle = (\Omega_m - i\Gamma_m)\delta_{m,n} - J_{n-1}\delta_{m,n-1} - J_n\delta_{m,n+1} - i(\Gamma_m\Gamma_n)^{1/2}e^{ik|d_{mn}|} \quad (16)$$

where Γ_m is the rate of spontaneous emission of the m-th qubit, d_{mn} is a distance between the m-th and the n-th qubits.

For three qubit chain the complex energies are derived by equating the matrix determinant $\langle n|H_{eff} - E|m\rangle$

$$\begin{pmatrix} \Omega_1 - i\Gamma_1 - E & -i\sqrt{\Gamma_1\Gamma_2}e^{ikd} - J & -i\sqrt{\Gamma_1\Gamma_3}e^{ik2d} \\ -i\sqrt{\Gamma_1\Gamma_2}e^{ikd} - J & \Omega_2 - i\Gamma_2 - E & -i\sqrt{\Gamma_3\Gamma_2}e^{ikd} - J \\ -i\sqrt{\Gamma_3\Gamma_1}e^{ik2d} & -i\sqrt{\Gamma_3\Gamma_2}e^{ikd} - J & \Omega_3 - i\Gamma_3 - E \end{pmatrix} \quad (17)$$

to zero.

For identical qubits ($\Omega_i = \Omega, \Gamma_i = \Gamma$) and long wavelength limit ($kd \ll 1$) we obtain from (17) the following matrix

$$\begin{pmatrix} \Omega - i\Gamma - E & -i\Gamma - J & -i\Gamma \\ -i\Gamma - J & \Omega - i\Gamma - E & -i\Gamma - J \\ -i\Gamma & -i\Gamma - J & \Omega - i\Gamma - E \end{pmatrix} \quad (18)$$

As is well known [12, 13], the energy spectrum of the effective Hamiltonian matrix (18) with $J = 0$ has a simple structure. There exists the only superradiant non-stationary state with the energy $E = \Omega - i3\Gamma$ and two degenerate stable states

with the energy $E = \Omega$. If J is different from zero the energy spectrum found from (18) is as follows:

$$\begin{aligned} E_1 &= \Omega - i\frac{3}{2}\Gamma - \sqrt{-\frac{9}{4}\Gamma^2 + 2J^2 + 4iJ\Gamma} \\ E_2 &= \Omega \\ E_3 &= \Omega - i\frac{3}{2}\Gamma + \sqrt{-\frac{9}{4}\Gamma^2 + 2J^2 + 4iJ\Gamma} \end{aligned} \quad (19)$$

Here, there are one stable and two unstable states. If J tends to zero we obtain from (19) two stable degenerate states and one unstable superradiant state. If the excitation frequency of a central qubit is different from that of other two qubits in a

chain we obtain from matrix determinant (18):

$$\begin{aligned} E_1 &= \Omega + \frac{1}{2}\Delta - i\frac{3}{2}\Gamma - \sqrt{\frac{1}{4}(\Delta - 3i\Gamma)^2 + 2i\Gamma\Delta + 2J^2 + 4iJ\Gamma} \\ E_2 &= \Omega \\ E_3 &= \Omega + \frac{1}{2}\Delta - i\frac{3}{2}\Gamma + \sqrt{\frac{1}{4}(\Delta - 3i\Gamma)^2 + 2i\Gamma\Delta + 2J^2 + 4iJ\Gamma} \end{aligned} \quad (20)$$

where $\Delta = \Omega_2 - \Omega$.

If $\Delta = J$ we obtain from (20):

$$\begin{aligned} E_1 &= \Omega - \Delta - i3\Gamma \\ E_2 &= \Omega \\ E_3 &= \Omega + 2\Delta \end{aligned} \quad (21)$$

IV. THREE QUBIT CHAIN UNDER THE INFLUENCE OF PULSED EXCITATION

Here we consider a time dependence of the excitation probability for every qubit, $\beta_n(t)$ in the chain subjected to pulsed

excitation. We start with the Hamiltonian, which describes the interaction of qubits with the photon field in a waveguide:

$$H = H_0 + \sum_k \omega_k a_k^\dagger a_k + \sum_{n=1}^3 \sum_k \left(\left(g_k^{(n)} e^{-ikx_n} \sigma_-^{(n)} \right) a_k^\dagger + h.c. \right) \quad (22)$$

where H_0 is given in (1).

The quantities $g_k^{(i)}$, ($i = 1, 2, 3$) in (22) describe the qubit interaction with the photon field in a waveguide:

$$g_k^{(i)} = \sqrt{\frac{\omega_k D_i^2}{2\hbar\epsilon_0 V}} \quad (23)$$

where D_i is a dipole moment of the i -th qubit, V is the effective volume of the photon-qubit interaction.

We will consider only single-photon states when one photon is present in the system and qubits are in the ground state,

or one of the qubits is excited, and there are no photons in the system. Following this, we write the state vector as follows:

$$|\Psi\rangle = \sum_{n=1}^3 \beta_n(t) e^{-i\Omega_n t} |n\rangle + \sum_k \gamma_k(t) e^{-i\omega_k t} |G, k\rangle \quad (24)$$

where $|1\rangle = |e_1 g_2 g_3 0_k\rangle$, $|2\rangle = |g_1 e_2 g_3 0_k\rangle$, $|3\rangle = |g_1 g_2 e_3 0_k\rangle$, $|G, k\rangle = |g_1 g_2 g_3, 1_k\rangle$.

The equations for the amplitudes $\gamma_k(t)$, $\beta_1(t)$, $\beta_2(t)$, $\beta_3(t)$ are derived from Schrodinger equation $i d|\Psi\rangle/dt = H|\Psi\rangle$.

$$\begin{aligned} \frac{d\beta_1}{dt} &= -i \sum_k g_k^{*(1)} g_k^{(1)} e^{ikx_1} e^{-i(\omega_k - \Omega_1)t} \tilde{\gamma}_k(0) - \sum_k |g_k^{(1)}|^2 \int_0^t \beta_1(t') e^{-i(\omega_k - \Omega_1)(t-t')} dt' \\ &\quad - \sum_k g_k^{*(1)} g_k^{(2)} e^{-ik(x_2 - x_1)} e^{i(\Omega_1 - \Omega_2)t} \int_0^t \beta_2(t') e^{-i(\omega_k - \Omega_2)(t-t')} dt' \\ &\quad - \sum_k g_k^{*(1)} g_k^{(3)} e^{-ik(x_3 - x_1)} e^{i(\Omega_1 - \Omega_3)t} \int_0^t \beta_3(t') e^{-i(\omega_k - \Omega_3)(t-t')} dt' \\ &\quad + iJ e^{i(\Omega_1 - \Omega_2)t} \beta_2 \end{aligned} \quad (25)$$

$$\begin{aligned}
\frac{d\beta_2}{dt} = & -i \sum_k g_k^{*(2)} e^{ikx_2} e^{-i(\omega_k - \Omega_2)t} \tilde{\gamma}_k(0) - \sum_k |g_k^{(2)}|^2 \int_0^t \beta_2(t') e^{-i(\omega_k - \Omega_2)(t-t')} dt' \\
& - \sum_k g_k^{*(2)} g_k^{(1)} e^{-ik(x_1 - x_2)} e^{i(\Omega_2 - \Omega_1)t} \int_0^t \beta_1(t') e^{-i(\omega_k - \Omega_1)(t-t')} dt' \\
& - \sum_k g_k^{*(2)} g_k^{(3)} e^{-ik(x_3 - x_2)} e^{i(\Omega_2 - \Omega_3)t} \int_0^t \beta_3(t') e^{-i(\omega_k - \Omega_3)(t-t')} dt' \\
& + iJ e^{i(\Omega_2 - \Omega_1)t} \beta_1 + iJ e^{i(\Omega_2 - \Omega_3)t} \beta_3
\end{aligned} \tag{26}$$

$$\begin{aligned}
\frac{d\beta_3}{dt} = & -i \sum_k g_k^{*(3)} e^{ikx_3} e^{-i(\omega_k - \Omega_3)t} \tilde{\gamma}_k(0) - \sum_k |g_k^{(3)}|^2 \int_0^t \beta_3(t') e^{-i(\omega_k - \Omega_3)(t-t')} dt' \\
& - \sum_k g_k^{*(3)} g_k^{(1)} e^{-ik(x_1 - x_3)} e^{i(\Omega_3 - \Omega_1)t} \int_0^t \beta_1(t') e^{-i(\omega_k - \Omega_1)(t-t')} dt' \\
& - \sum_k g_k^{*(3)} g_k^{(2)} e^{-ik(x_2 - x_3)} e^{i(\Omega_3 - \Omega_2)t} \int_0^t \beta_2(t') e^{-i(\omega_k - \Omega_2)(t-t')} dt' \\
& + iJ e^{i(\Omega_3 - \Omega_2)t} \beta_2
\end{aligned} \tag{27}$$

$$\begin{aligned}
\gamma_k(t) = & \tilde{\gamma}_k(0) - ig_k^{(1)} e^{-ikx_1} \int_0^t \beta_1(t') e^{i(\omega_k - \Omega_1)t'} dt' \\
& - ig_k^{(2)} e^{-ikx_2} \int_0^t \beta_2(t') e^{i(\omega_k - \Omega_2)t'} dt' - ig_k^{(3)} e^{-ikx_3} \int_0^t \beta_3(t') e^{i(\omega_k - \Omega_3)t'} dt'
\end{aligned} \tag{28}$$

Here $\tilde{\gamma}_k(0) = \sqrt{2/L} \gamma_k(0)$ where L is a waveguide length, and $\gamma_k(0)$ is the initial Gaussian envelope:

$$\gamma_k(0) = \left(\frac{2}{\pi \Delta_k^2} \right)^{1/4} \exp \left(i(k - k_s)x_0 - \frac{(k - k_s)^2}{\Delta_k^2} \right) \tag{29}$$

where Δ_k is a spectral width of the packet in k space, which is related to a spatial width of the packet: $\sigma = \sqrt{2}/\Delta_k$, $-x_0$ is the position of the maximum of envelope curve on x -axis at the initial moment of time, $k_s = \omega_s/v_g$ is the center of the wave packet in the k space, ω_s is the frequency of the center of the photon pulse, v_g is the group velocity of the wave in a waveguide.

In the framework of the single-photon approximation, the

system of equations (25, 26, 27) is accurate. A further simplification of this system is associated with the Wigner-Weisskopf approximation, which allows us to express the photon-qubit interaction couplings $g_k^{(i)}$ in terms of the rate of spontaneous decay, Γ_i of the i -th qubit into the waveguide, (see the appendix).

$$\Gamma_i = 4L \left| g^{(i)}(\Omega) \right|^2 / v_g \tag{30}$$

As is shown in the appendix, in the Wigner-Weisskopf approximation, equations (25, 26, 27) for the excitation amplitudes, $\beta_n(t)$ can be written in the following form:

$$\begin{aligned}
\frac{d\beta_1}{dt} = & -i \sqrt{\frac{\Gamma_1 v_g}{4\pi}} \left(\frac{\omega_s}{\Omega_1} \right)^{1/2} \exp(i\Omega_1 t) f(k_s, x_1, t) - \frac{\Gamma_1}{2} \beta_1(t) + iJ e^{i(\Omega_1 - \Omega_2)t} \beta_2(t) \\
& - \frac{\sqrt{\Gamma_1 \Gamma_2}}{2} \sqrt{\frac{\Omega_2}{\Omega_1}} e^{-ik_2 d} e^{i(\Omega_1 - \Omega_2)t} \beta_2(t) - \frac{\sqrt{\Gamma_1 \Gamma_3}}{2} \sqrt{\frac{\Omega_3}{\Omega_1}} e^{-ik_3 2d} e^{i(\Omega_1 - \Omega_3)t} \beta_3(t)
\end{aligned} \tag{31}$$

$$\begin{aligned}
\frac{d\beta_2}{dt} = & -i \sqrt{\frac{\Gamma_2 v_g}{4\pi}} \left(\frac{\omega_s}{\Omega_2} \right)^{1/2} \exp(i\Omega_2 t) f(k_s, x_2, t) - \frac{\Gamma_2}{2} \beta_2(t) \\
& - \frac{\sqrt{\Gamma_2 \Gamma_1}}{2} \sqrt{\frac{\Omega_1}{\Omega_2}} e^{ik_1 d} e^{i(\Omega_2 - \Omega_1)t} \beta_1(t) - \frac{\sqrt{\Gamma_2 \Gamma_3}}{2} \sqrt{\frac{\Omega_3}{\Omega_2}} e^{-ik_3 d} e^{i(\Omega_2 - \Omega_3)t} \beta_3(t) \\
& + iJ e^{i(\Omega_2 - \Omega_1)t} \beta_1(t) + iJ e^{i(\Omega_2 - \Omega_3)t} \beta_3(t)
\end{aligned} \tag{32}$$

$$\begin{aligned}
\frac{d\beta_2}{dt} = & -i\sqrt{\frac{\Gamma_2 v_g}{4\pi}} \left(\frac{\omega_s}{\Omega_2}\right)^{1/2} \exp(i\Omega_2 t) f(k_s, x_2, t) - \frac{\Gamma_2}{2} \beta_2(t) \\
& - \frac{\sqrt{\Gamma_2 \Gamma_1}}{2} \sqrt{\frac{\Omega_1}{\Omega_2}} e^{ik_1 d} e^{i(\Omega_2 - \Omega_1)t} \beta_1(t) - \frac{\sqrt{\Gamma_2 \Gamma_3}}{2} \sqrt{\frac{\Omega_3}{\Omega_2}} e^{-ik_3 d} e^{i(\Omega_2 - \Omega_3)t} \beta_3(t) \\
& + iJ e^{i(\Omega_2 - \Omega_1)t} \beta_1(t) + iJ e^{i(\Omega_2 - \Omega_3)t} \beta_3(t)
\end{aligned} \tag{33}$$

where the quantity $f(k_s, x, t)$ is the harmonic filled Gaussian envelope in real space:

$$f(k_s, x, t) = (2\pi\Delta_k^2)^{1/4} \exp\left(ik_s(x - v_g t) - \frac{\Delta_k^2}{4}(x_0 + x - v_g t)^2\right) \tag{34}$$

It can be expressed in terms of Gaussian envelope $\gamma_k(0)$ (29) in the k space:

$$f(k_s, x, t) = \int_{-\infty}^{\infty} dk \gamma_k(0) e^{ik(x - v_g t)} \tag{35}$$

V. NUMERICAL CALCULATIONS OF THE QUBITS EXCITATION AMPLITUDES, $\beta_n(t)$

Below, we present the results of numerical calculations of the excitation amplitudes of a system of three qubits where the interaction between the nearest neighbors is taken into account. We solve the differential equations (31, 32, 33) with the initial conditions: $\beta_i(0) = 0$, ($i = 1, 2, 3$), with the harmonic filled Gaussian envelope (34) at the initial moment of time, $f(k_s, x, 0)$. In this case, the width of the initial Gaussian packet Δ_k in (29) was chosen to ensure a maximum of the excitation amplitude upon excitation of a *single* qubit. As was shown in [4] it can be achieved if $\Delta_k = \Gamma/v_g$. For the values $\Gamma/2\pi = 10$ MHz, $v_g = 10^8$ m/c we obtain $\Delta_k = 0.21$ m⁻¹. The time which takes for the center of the Gaussian envelope to reach the first qubit in the chain was chosen to exceed the spontaneous decay of the qubit excitation into the waveguide, $2/\Gamma$. Therefore, we take $x_0 = 10v_g/\Gamma \approx 47.74$ m. In all plots the time is normalized to $\tau = 1/\Gamma = 1.59 \times 10^{-8}$ s.

A. The excitation of identical qubits

Figure 2 shows the spectroscopy calculated according to equations (31, 32, 33) of the maximum values of the excitation probabilities of each qubit depending on the excitation frequency of the external signal ω_s . The calculations were carried out for identical qubits for $d = 1$ mm, $J/\Omega = 0.05$, $\Omega/2\pi = 5$ GHz, $\Gamma/2\pi = 10$ MHz.

For these values we obtain from the determinant (17) the complex energies:

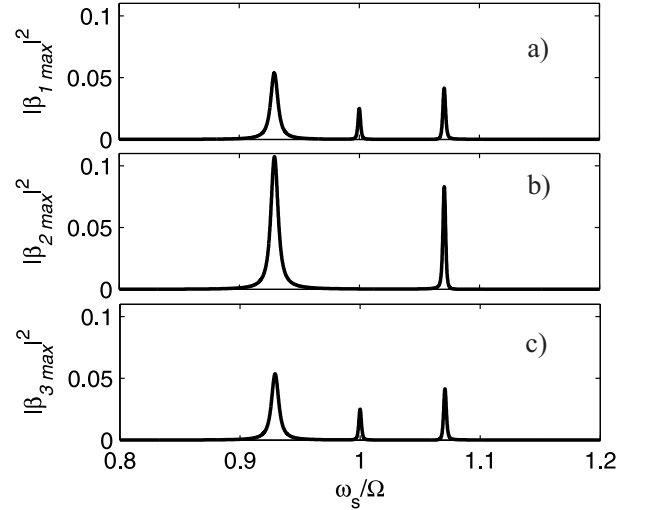


FIG. 2: Spectroscopy of a three-qubit system. The dependence of the maximum excitation probability of the qubits on the single-photon probing frequency ω_s . $d = 1$ mm, $J/\Omega = 0.05$, $\Omega/2\pi = 5$ GHz, $\Gamma/2\pi = 10$ MHz.

$$\begin{aligned}
E_1/\Omega & \approx 0.9293 - i5.82 \times 10^{-3} \\
E_2/\Omega & \approx 1 \\
E_3/\Omega & \approx 1.0707 - i1.71 \times 10^{-4}
\end{aligned} \tag{36}$$

Therefore, the first level has maximal width. The width of the third level is less, while the width of the second level is theoretically zero if inter qubit space, $d = 0$. For $d = 1$ mm we used in the calculations, the width of the second level is much less than those of the other ones. These features are clearly seen in Fig.2. The peak positions and their widths are well correlated with the real and imaginary parts of (36). Moreover, the peak heights are also well corresponded with the squared values of the superposition coefficients $|c_n^{(i)}|^2$ in the collective wave functions (8, 9, 10).

For instance, if the probe frequency ω_s is equal to E_1 , the relative values of the peak heights (left peaks in Fig.2) are similar to those of superposition coefficients in (8) with the amplitudes of the first and the third qubits being equal, while

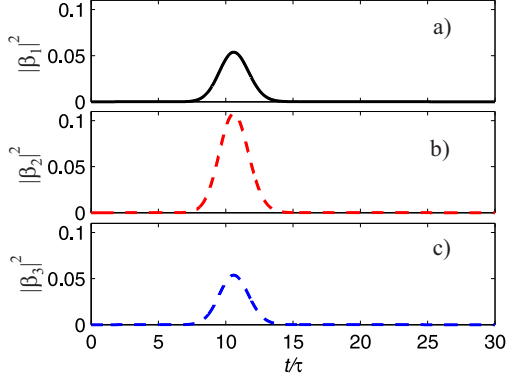


FIG. 3: The time evolution of the qubits excitation probabilities $|\beta_n(t)|^2$, when the probe frequency is tuned to the first energy level $\omega_s = ReE_1 = 0.9293\Omega$, $d = 1\text{mm}$, $J/\Omega = 0.05$, $\Omega/2\pi = 5\text{GHz}$, $\Gamma/2\pi = 10\text{MHz}$.

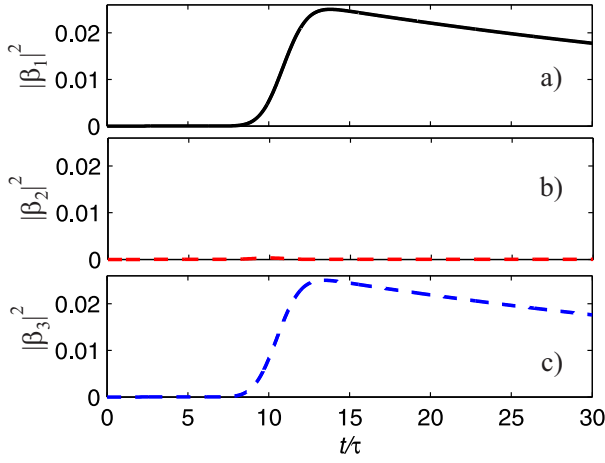


FIG. 4: The time evolution of the qubits excitation probabilities $|\beta_n(t)|^2$, when the probe frequency is tuned to the second energy level $\omega_s = ReE_2 = \Omega$, $d = 1\text{mm}$, $J/\Omega = 0.05$, $\Omega/2\pi = 5\text{GHz}$, $\Gamma/2\pi = 10\text{MHz}$.

the amplitude of the second qubit is $\sqrt{2}$ times more. If the probe frequency is equal to E_2 (central peaks in Fig.2), the probability amplitude for the excitation of the second qubit (panel b) in Fig.2) is zero, which agrees with (8b).

The time evolution of the qubits excitation probabilities $|\beta_n(t)|^2$, when the probe frequency is tuned, respectively, to first, second, and third energy levels (see (36) is shown in Figs.3, 4, 5.

As is seen in these figures, the relative value of the amplitudes agrees with the contribution of a given qubit in the superposition functions (8, 9, 10). For instance, the excitation amplitude of the central qubit in Fig.4 is equal to zero, because its contribution in a wavefunction (9) is also equal to zero. The time dependence of the amplitudes corresponds with the widths of relevant resonances in (36). For example, the first level E_1 has the maximum width. Therefore, as is

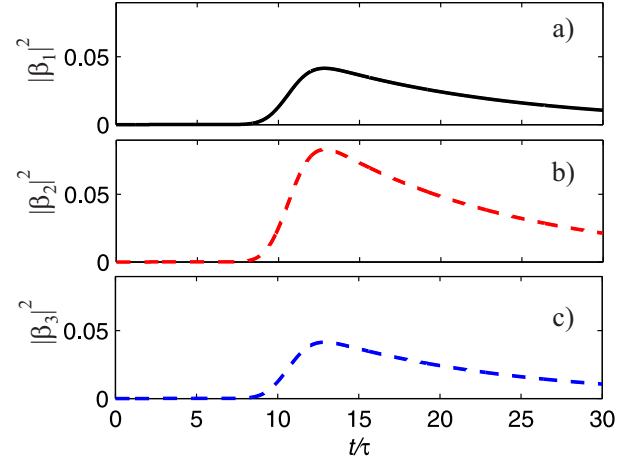


FIG. 5: The time evolution of the qubits excitation probabilities $|\beta_n(t)|^2$, when the probe frequency is tuned to the third energy level $\omega_s = ReE_3 = 1.0707\Omega$, $d = 1\text{mm}$, $J/\Omega = 0.05$, $\Omega/2\pi = 5\text{GHz}$, $\Gamma/2\pi = 10\text{MHz}$.

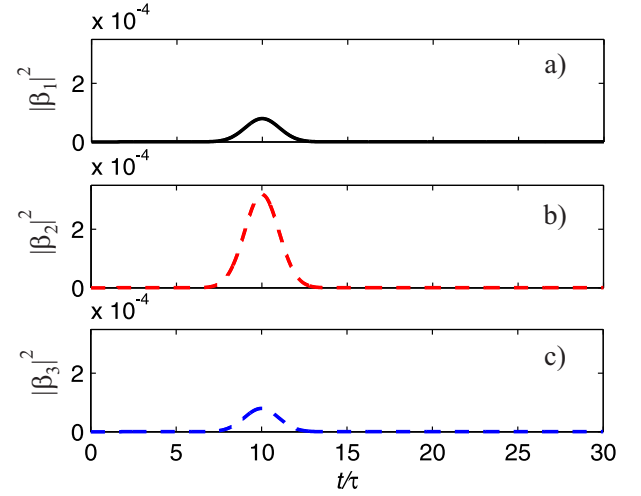


FIG. 6: The time evolution of the qubits excitation probabilities $|\beta_n(t)|^2$, when the probe frequency is tuned to the second energy level $\omega_s = ReE_2 = \Omega$, $d = 0$, $J/\Omega = 0.05$, $\Omega/2\pi = 5\text{GHz}$, $\Gamma/2\pi = 10\text{MHz}$.

seen in Fig.3, the excitation amplitudes for every qubit rapidly decay. The width of the third level E_3 is much less than that of the first one. If the probe frequency is tuned to the frequency of the third level, it results in a slow decay of the excitation amplitudes (see Fig.5). Much slower decay is observed if the probe frequency is tuned to the second level E_2 (see Fig 4). As we pointed out before, the width of the second level E_2 is only due to the non zero value of d . For $d = 1\text{mm}$, which we used in the calculations, this width is quite small resulting in a very slow decay of the amplitudes in Fig.4. We attribute this slow decay to solely the interference effects due to the finite distance between qubits. If we assume $d = 0$ in equations (31, 32, 33), the probability of the qubit excitation is greatly reduced (see Fig.6).

TABLE I: The resonances and relevant superposition coefficients for $J/\Omega = 0.05$, $\Gamma/2\pi = 10$ MHz, $d = 1$ mm.

E_j/Ω	$c_1^{(j)}$	$c_2^{(j)}$	$c_3^{(j)}$
$0.9907 - 0.004683i$	0.7004	$0.1370 + 0.00475i$	0.7004
$0.9996 - 0.000437i$	0.7071	0.0000	-0.7071
$1.5097 - 0.001273i$	$0.09686 + 0.00336i$	-0.9906	$0.09686 + 0.00336i$

B. Excitation of non identical qubits

Below, we consider the excitation of the three-qubit chain when the excitation frequency of one of the qubit is different from that of the other two qubits. Therefore, we take the first and the third qubit as identical ($\Omega_1 = \Omega_3 = \Omega$), while the excitation frequency of the second qubit is Ω_2 . We also assume

all the rates of spontaneous emission as identical ($\Gamma_i = \Gamma$). First, we consider the case of large detuning when $\Delta/\Omega = 0.5$ ($\Omega_2/\Omega = 1.5$). The calculated values of resonances and relevant superposition coefficients found from the Hamiltonian matrix (17) for $J/\Omega = 0.05$, $\Gamma = 10$ MHz, $d = 1$ mm are presented in Table I.

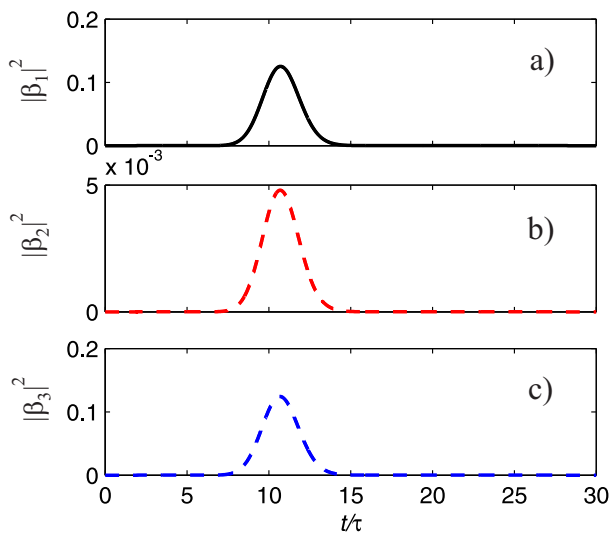


FIG. 7: The time evolution of the qubits excitation probabilities $|\beta_n(t)|^2$, when the probe frequency is tuned to the first resonance $\omega_s = \text{Re } E_1 = 0.9903\Omega$, $d = 1$ mm, $J/\Omega = 0.05$, $\Omega/2\pi = 5$ GHz, $\Gamma/2\pi = 10$ MHz, $\Delta/\Omega = 0.5$ ($\Omega_2/\Omega = 1.5$).

As can be seen from this table, the values of the superposition coefficients correlate well with the asymptotic behavior of expressions (14, 15) for $\Delta/J \gg 1$.

The time dependence of the excitation amplitudes at the frequency of the first resonance ($\text{Re } E_1/\Omega = 0.9907$) is shown in Fig.7. The excitation amplitudes of the first and second qubits are the same, and the central qubit is practically not excited. Since this resonance has a relatively large width, the amplitudes decay relatively quickly.

When excited at the frequency of the second resonance ($\text{Re } E_2/\Omega = 0.9996$), whose width is quite small, we see a subradiant mode when the first and third qubits are excited (Fig.8), and the central qubit is practically not excited (see

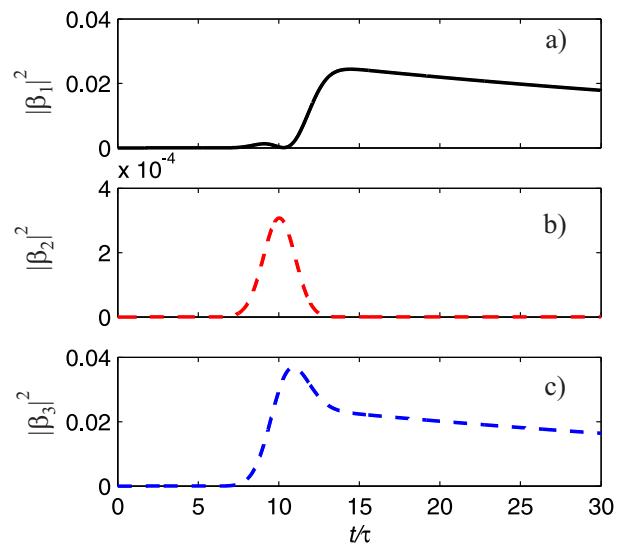


FIG. 8: The time evolution of the qubits excitation probabilities $|\beta_n(t)|^2$, when the probe frequency is tuned to the second resonance $\omega_s = \text{Re } E_2 = 0.9999\Omega$, $d = 1$ mm, $J/\Omega = 0.05$, $\Omega/2\pi = 5$ GHz, $\Gamma/2\pi = 10$ MHz, $\Delta/\Omega = 0.5$ ($\Omega_2/\Omega = 1.5$).

Table I).

When excited at the frequency of the third resonance ($\text{Re } E_3/\Omega = 1.51$), the second qubit is mainly excited (Fig.9), since the contributions of the first and third qubits to the wave function of the third level are relatively small (see the last line in Table I).

1. Excitation of non identical qubits with $\Delta = J$

In the last part of this section we consider the dynamics of the excitation of a three-qubit system for $\Delta = J$. It corresponds to the point of intersection of the graphs in panel a) in

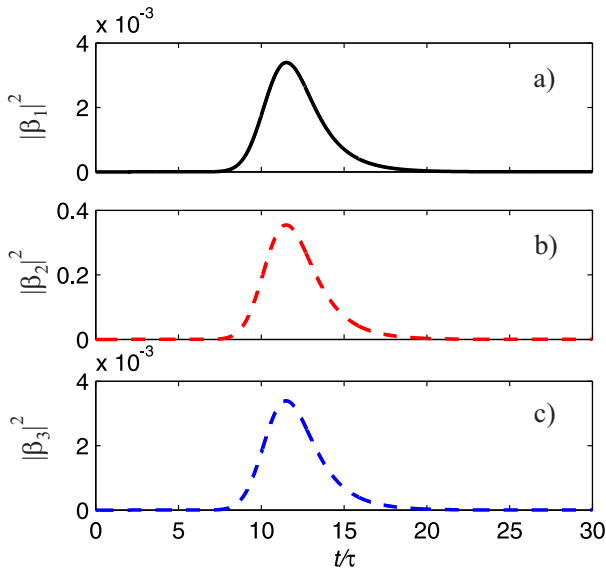


FIG. 9: The time evolution of the qubits excitation probabilities $|\beta_n(t)|^2$, when the probe frequency is tuned to the third resonance $\omega_s = \text{Re } E_3 = 1.5\Omega$, $d = 1$ mm, $J/\Omega = 0.05$, $\Omega/2\pi = 5\text{GHz}$, $\Gamma/2\pi = 10$ MHz, $\Delta/\Omega = 0.5$ ($\Omega_2/\Omega = 1.5$)

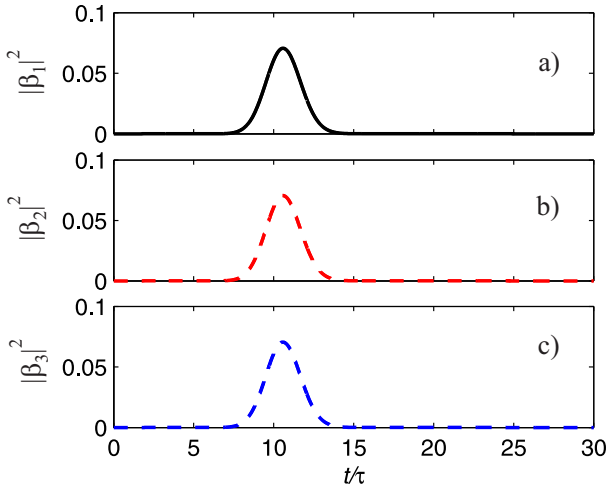


FIG. 10: The time evolution of the qubits excitation probabilities $|\beta_n(t)|^2$, when the probe frequency is tuned to the first resonance $\omega_s = \text{Re } E_1 = 0.95\Omega$, $d = 1$ mm, $J/\Omega = 0.05$, $\Omega/2\pi = 5\text{GHz}$, $\Gamma/2\pi = 10$ MHz, $\Delta/\Omega = 0.05$ ($\Omega_2/\Omega = 1.05$).

Fig.1. In this case, the state with the lowest energy has a finite width (see first equation in (21), and, as indicated above, the corresponding wave function of the stationary state has the maximum entanglement. The dynamics of the excitation of this state is shown in Fig.10. The amplitudes of the excitation of qubits are the same and decay quickly enough.

The second energy level of this system has practically no width (second line in (21). Besides, as follows from (8b), the contribution of the second qubit to this state is zero. These features are presented in Fig.11. As can be seen from this figure, the contribution of the second qubit is quite small, while

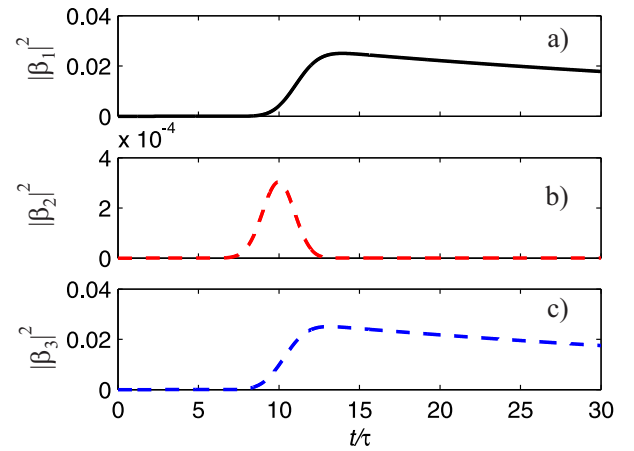


FIG. 11: The time evolution of the qubits excitation probabilities $|\beta_n(t)|^2$, when the probe frequency is tuned to the second resonance $\omega_s = \text{Re } E_2 = 1.0\Omega$, $d = 1$ mm, $J/\Omega = 0.05$, $\Omega/2\pi = 5\text{GHz}$, $\Gamma/2\pi = 10$ MHz, $\Delta/\Omega = 0.05$ ($\Omega_2/\Omega = 1.05$).

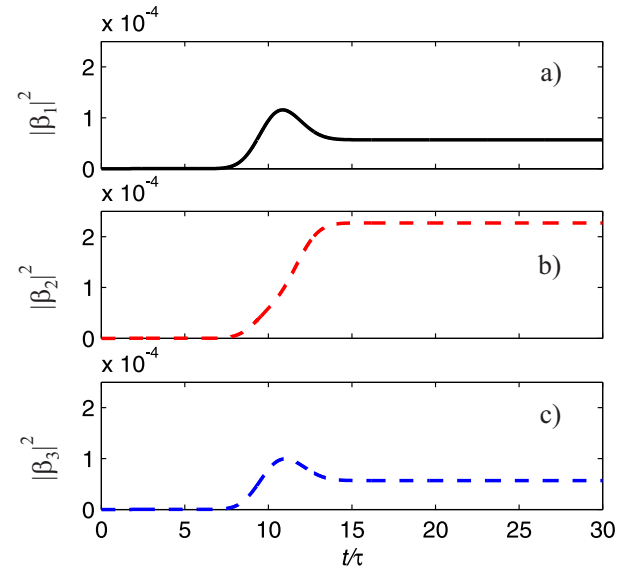


FIG. 12: The time evolution of the qubits excitation probabilities $|\beta_n(t)|^2$, when the probe frequency is tuned to the third resonance $\omega_s = \text{Re } E_3 = 1.1\Omega$, $d = 1$ mm, $J/\Omega = 0.05$, $\Omega/2\pi = 5\text{GHz}$, $\Gamma/2\pi = 10$ MHz, $\Delta/\Omega = 0.05$ ($\Omega_2/\Omega = 1.05$).

the damping of the excitation amplitudes of the first and third qubits is rather slow.

From Fig.12, it follows that the amplitudes excitations of qubits of the third energy level (last line in equation (21) are quite small, although the presence of undamped subradiant states with almost zero width is seen.

VI. CONCLUSION

In summary, we have proposed the experimentally achievable method for the characterization of the collective states

of qubits in a linear chain. The method is based on measuring the time evolution of the probability of excitation of qubits using a conventional control pulse technique, which is widely used for recording and reading out the information in qubit systems. We have examined this method for a three-qubit linear chain with the nearest neighbor Ising interaction between qubits. We have shown that the excitation of qubits by a Gaussian pulse with harmonic filling allows us to determine the energies, their widths, and the wave functions of the corresponding collective states. The extension of this method to more qubits in a chain is straightforward.

Acknowledgments

Ya. S. G. acknowledges A. N. Sultanov for fruitful discussions. The work is supported by Ministry of Science and Higher Education of the Russian Federation under Project

Appendix

1. Wigner-Weisskopf approximation for the dynamical equations (25, 26, 27)

The main assumption is that the quantities $\beta_i(t)$ under integrals in (25, 26, 27) are slow functions of time as compared to those in the exponents. Therefore, for times $t_1 \ll t$ the integrand oscillates very rapidly and there is no significant contribution to the value of the integral. The most dominant contribution originates from times $t_1 \approx t$. We therefore evaluate

$\beta_i^{(t)}$ at the actual time t and move it out of the integrand. In this limit, the decay becomes a memoryless process (Markov process). To evaluate the remaining integral in the right hand side of (A.1) we extend the upper integration limit to infinity since there is no significant contribution for $t_1 \gg t$. Therefore, we obtain:

$$\int_0^t \beta_i(t') e^{-i(\omega_k - \Omega_i)(t-t')} dt' \approx \beta_i(t) \int_0^t e^{-i(\omega_k - \Omega_i)(t-t')} dt' \quad (\text{A.1})$$

$$\int_0^t e^{-i(\omega_k - \Omega_i)(t-t')} dt' \approx \int_0^\infty e^{-i(\omega_k - \Omega_i)(t-t')} dt' \quad (\text{A.2})$$

The last integral is known to be:

$$\int_0^\infty e^{-i(\omega_k - \Omega_i)(t-t')} dt' = \pi \delta(\omega_k - \Omega_i) - iP \left(\frac{1}{\omega_k - \Omega_i} \right) \quad (\text{A.3})$$

where P represents the Cauchy principal part, which leads to a frequency shift. In what follows, we do not write explicitly this shift, which is assumed to be included in the qubit frequency. Therefore, the second terms in the equations (25, 26, 27) can be rewritten as follows:

$$\sum_k |g_k^{(i)}|^2 \int_0^t \beta_i(t') e^{-i(\omega_k - \Omega_i)(t-t')} dt' = \beta_i(t) \pi \sum_k |g_k^{(i)}|^2 \delta(\omega_k - \Omega_i) \equiv \beta_i(t) \frac{\Gamma_i}{2} \quad (\text{A.4})$$

Next, we apply the same procedure to cross terms in (25, 26, 27).

$$\begin{aligned} & \sum_k g_k^{(i)} g_k^{(j)*} e^{ik(x_i - x_j)} e^{i(\Omega_i - \Omega_j)t} \int_0^t \beta_j(t') e^{-i(\omega_k - \Omega_j)(t-t')} dt' \\ &= \sum_k g_k^{(i)} g_k^{(j)*} e^{ik(x_i - x_j)} e^{i(\Omega_i - \Omega_j)t} \beta_j(t) \pi \delta(\omega_k - \Omega_j) \end{aligned} \quad (\text{A.5})$$

In (A.4) the quantity Γ_i is the rate of spontaneous emission for the i -th qubit.

$$\Gamma_i = 2\pi \sum_k |g_k^{(i)}|^2 \delta(\omega_k - \Omega_i) \quad (\text{A.6})$$

In a one dimensional case the summation over k is replaced by the integration:

$$\sum_k \Rightarrow 2 \frac{L}{2\pi} \int_{-\infty}^{\infty} dk = \frac{L}{2\pi} 4 \int_0^{\infty} d|k| = \frac{2L}{\pi v_g} \int_0^{\infty} d\omega_k \quad (\text{A.7})$$

where the factor of 2 arises from summing over the two polarization states associated with each k -vector, and we take a linear frequency dispersion $\omega_k = v_g |k|$ well above the cutoff frequency of a waveguide.

Applying the prescription (A.7) to (A.6) we express the coupling $g_{\Omega_i}^{(i)}$ at the qubit resonance frequency Ω_i in terms of the rate of spontaneous emission Γ_i :

$$|g_{\Omega_i}^{(i)}|^2 = \frac{\Omega_i D_i^2}{2\hbar \epsilon_0 V} \equiv \frac{\Gamma_i v_g}{4L} \quad (\text{A.8})$$

With the use of (A.7) and (A.8) we write the last line in (A.5) in the following form:

$$\begin{aligned} & \sum_k g_k^{(i)} g_k^{(j)*} e^{ik(x_i-x_j)} e^{i(\Omega_i-\Omega_j)t} \beta_j(t) \pi \delta(\omega_k - \Omega_j) \\ &= \frac{\sqrt{\Gamma_i \Gamma_j}}{2} \left(\frac{\Omega_j}{\Omega_i} \right)^{1/2} e^{i\frac{\Omega_j}{c}(x_i-x_j)} e^{i(\Omega_i-\Omega_j)t} \beta_j(t) \end{aligned} \quad (\text{A.9})$$

Now we pay attention to the first terms in the right hand

sides of Eqs. 25, 26, 27. The initial wave packet $\tilde{\gamma}_k(0)$ must be normalized to unity:

$$\sum_k |\tilde{\gamma}_k(0)|^2 = \frac{\pi}{L} \sum_k |\gamma_k(0)|^2 = \frac{\pi}{L} 2 \frac{L}{2\pi} \int_{-\infty}^{\infty} |\gamma_k(0)|^2 dk = 1 \quad (\text{A.10})$$

The Gaussian envelope $\gamma_k(0)$ defined in (29) automatically satisfies this condition:

$$\begin{aligned} -i \sum_k g_k^{(i)} \tilde{\gamma}_k(0) e^{ikx_i} e^{-i(\omega_k-\Omega_i)t} &= -i \sqrt{\frac{\Gamma_i v_g}{4L}} \sqrt{\frac{\omega_s}{\Omega_i}} \frac{L}{2\pi} 2 \sqrt{\frac{\pi}{L}} \int_{-\infty}^{\infty} dk \gamma_k(0) e^{ikx_i} e^{-i(\omega_k-\Omega_i)t} \\ &= -i \sqrt{\frac{\Gamma_i v_g}{4\pi}} \sqrt{\frac{\omega_s}{\Omega_i}} \int_{-\infty}^{\infty} dk \gamma_k(0) e^{ikx_i} e^{-i(\omega_k-\Omega_i)t} \end{aligned} \quad (\text{A.11})$$

where ω_s is the external excitation frequency.

Integral in (A.11) of Gaussian envelope can be analytically calculated which results in the system of linear differential equations (31, 32, 33) from the main text.

It is noteworthy that the waveguide length L does not explicitly enter in these equations. It implicitly enters only in the definition of Γ_i in (A.8) the value of which is taken from experiments.

-
- [1] Y. Wang, J. Minar, L. Sheridan, and V. Scarani, Phys. Rev. A83, 063842 (2011).
 - [2] M. Stobinska G. Alber, and G. Leuchs, Europhys. Lett. 86, 14007 (2009).
 - [3] E. Rephaeli, J.-T. Shen, and S. Fan, Phys. Rev. A82, 033804 (2010).
 - [4] Y. Chen, M. Wubs, J. Mrk, and A. F. Koendrink, New J. Phys. 13, 103010 (2011).
 - [5] P. Domokos, P. Horak, and H. Ritsch, Phys. Rev A65, 033832 (2002).
 - [6] S. Derouault, M.A. Bouchene, Phys. Lett. A376, 3491 (2012).
 - [7] J.-F. Huang, J.-Q. Liao, and C. P. Sun, Phys. Rev. A87, 023822 (2013).
 - [8] S. Derouault and M. A. Bouchene, Phys. Rev. A90, 023828 (2014).
 - [9] Ya. S. Greenberg, A. A. Shtygashev, Physics of the Solid State. 60, 2109 (2018).
 - [10] The impressive list of currently existing superconducting quantum processors is available at https://en.wikipedia.org/wiki/List_of_quantum_processors.
 - [11] Z. Liao, X. Zeng, Shi-Yao Zhu, and M. S. Zubairy, Phys. Rev. A92, 023806 (2015).
 - [12] Ya. S. Greenberg and A. A. Shtygashev, Phys. Rev. A 92, 063835 (2015).
 - [13] A. Volya and V. Zelevinsky, Exploring quantum dynamics in an open many-body system: transition to superradiance. J. Opt. B: Quantum Semiclass. Opt. 5, S450 (2003).